Int. J. Heat Mass Transfer. Vol. 26, No. 1, pp. 87–99, 1983
Printed in Great Britain

0017-9310/83/010087-13 $03.00/0

A UNIT CELL MODEL FOR PREDICTING THE THERMAL CONDUCTIVITY OF A GRANULAR MEDIUM CONTAINING AN ADHESIVE BINDER

K. W. JACKSON
Bell Telephone Laboratories, Atlanta, GA 30071, U.S.A.

and

W. Z. BLACK
School of Mechanical Engineering, Georgia Institute of Technology, Atlanta, GA 30332, U.S.A.

(*Received* 30 *October* 1981 *and in revised form* 1 *June* 1982)

Abstract—A unit cell model is proposed which can be used to predict the effective thermal conductivity of a granular medium composed of sand particles, a thermal binder, and air. The unit cell model is described by three dominant thermal conductances which account for the heat transport across the interfaces among the components comprising the medium. The stereological concept of contiguity is used to quantitatively link the macroscopic effective thermal conductivity to the microscopic interfacial contact area among the components. Utilizing a geometric model of a representative contact between two particles, an analytical expression for the contiguity is developed. This expression is used in the unit cell model to calculate the effective thermal conductivity of the medium as a function of the thermal conductivity of the components and their volumetric concentration. The predictive accuracy of the unit cell model for sand-like media is verified with numerous quantitative microscopic measurements and thermal conductivity data obtained with the transient, cylindrical probe technique.

The unit cell model is applied to the design of thermal backfill materials. Both analysis and experiment demonstrate that thermally coupling contiguous sand particles with a binder can significantly increase the effective thermal conductivity of dry sand. Four basic microstructure regimes of the medium are identified, and these regimes are quantitatively related to the volume fraction of the binder. The greatest increase in the effective thermal conductivity with respect to the volume fraction of the binder is shown to occur in a regime where the sand particles become thermally coupled with the binder. The unit cell model identifies quantitative guidelines for the thermal conductivity and volume fraction of the binder that can be used to produce the greatest increase in the effective thermal conductivity of dry sand. Thus, the results of this study have practical application to the design and development of thermal backfill materials for increasing the heat transfer between the earth and underground heat sources such as buried electric power cables and ground source heat pump coils.

NOMENCLATURE

A_{zz}, area of interparticle contact;
C_{ij}, contiguity between component i and j or fraction of the total interface area of i that shares a common interface area with j;
k, thermal conductivity;
K, thermal conductance;
N, number of contacts per particle;
q', heat transfer rate per unit length;
r_c, radius of particle contact, Fig. 4;
$(P_L)_{ij}$, number of i–j intersections encountered per unit length of test line on a section of microstructure;
S, interface area per unit volume;
t, time;
t_f, thickness of binder film layer;
V, volume;
X, dimensions of the unit cell model, Fig. 3.

Greek symbols
ϕ, volume fraction;
ψ, wetting angle, Fig. 4;
θ, temperature rise above ambient;
η, efficiency of thermal coupling.

Subscripts
α, particle property;
β, binder property;
γ, air property;
c, limiting value for meniscus structure;
d, value for medium without binder;
e, effective value;
f, film structure;
T, total value.

INTRODUCTION

THE EFFECTIVE thermal conductivity of granular media is a key property which can significantly influence the design and performance of a system which must dissipate heat to or extract heat from these materials. For example, heat transfer rates from buried high voltage power transmission cables, ground source heat

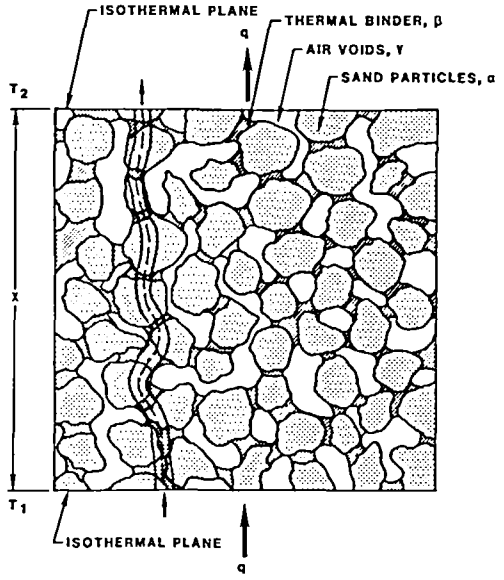

FIG. 1. Cross-section showing the microstructure of a three component granular material composed of sand particles, α, thermal binder, β, and air voids, γ.

pump coils and oil pipelines depend primarily upon the effective thermal conductivity of the soil which often consists of sand-like particles, cemented together with a binder of water, or clay particles or both. In the foundry industry the effective thermal conductivity of molding sand can affect not only the surface quality of the castings, but also their physical properties.

This paper contributes to the solution of predicting the effective thermal conductivity of a macroscopically isotropic granular medium having the structural arrangement illustrated in Fig. 1. The medium is comprised of sand-like particles, α, an adhesive binder, β, and air voids, γ. The particle size is assumed to be about 0.1–2 mm. The binder is assumed to be concentrated at the particle contacts and to occupy a volumetric concentration less than about 10% of that of the composite. A unit cell model is proposed which can be used to predict the effective thermal conductivity of the composite as a function of the thermal conductivity of the components, their volumetric concentration, and the effective thermal conductivity of the granular medium at zero concentration of binder.

Although considerable theoretical and experimental research has been conducted on the effective thermal conductivity of granular media, relatively few studies have been directed to the type of structure illustrated in Fig. 1. This lack of interest is somewhat surprising because the effective thermal conductivity of a granular medium having this structure is extremely sensitive to the binder concentration, especially at the lower binder concentrations. Moreover, few studies have attempted to quantitatively relate the structure of a granular medium to its effective thermal conductivity.

Previous research [1–5] indicates that the structure of a granular medium exerts a dominant influence on its effective thermal conductivity. Specifically, the effective thermal conductivity of a composite will be greatest when the component having the highest thermal conductivity forms a continuous matrix, interspersed with the discrete, lower thermal conductivity components. For example, because low thermal conductivity air essentially forms the continuous matrix in dry sands, these materials are relatively good thermal insulators. However, thermally coupling the sand particles with a small amount of binder such as water, with thermal conductivity greater by a factor of about 25 than that of air, produces a dramatic increase in the effective thermal conductivity of the composite. In fact, de Vries' data [5] for moist sand show that a 10% volume concentration of water increases the effective thermal conductivity of dry sand by about a factor of eight. Thus, an effort to physically model the effective thermal conductivity of a granular medium containing a binder must include a detailed analysis of the thermal coupling between adjacent particles. This in turn necessitates a quantitative description of the interfacial boundary conditions among the components comprising the medium. Existing models, however, have largely ignored this problem. Therefore there is no adequate model to quantitatively describe the efficiency of the interparticle thermal coupling as a function of the thermal conductivity and volume fraction of the binder and air.

THEORETICAL ANALYSIS

Energy transport through the medium illustrated in Fig. 1 occurs by conduction, convection and radiation; however, conduction is the dominant mode in a dry, sand-like granular medium with an average temperature of 298 K. The convective contribution to the total energy transport is negligible because of the small size of the intergranular pore spaces whereas the radiative contribution is negligible because of the relatively low absolute temperature of the medium.

When conduction is the dominant mechanism of energy transport through the medium, the determination of the temperature distribution and the heat flow can be approached by two basic methods. The first method involves solving the heat conduction equation exactly (at least in principle) within each region of the medium giving the temperature distribution and the heat flow.

An alternate method to the exact approach is to approximate the real medium with an equivalent homogeneous medium which gives the same average temperature distribution and heat flux. The distributed properties of the original medium are thus lumped into effective properties of an equivalent homogeneous system and the heat conduction equation for the homogeneous medium is solved.

An exact solution is impractical due to an inherent lack of information about the size, shape, and spatial

distribution of the particles; therefore, the approximate solution of the equivalent homogeneous medium is justified. The approximate method of the equivalent homogeneous medium, however, is restricted to macroscopic material volumes that contain a large number of particles because only then are the effective properties experimentally well-defined.

The material properties necessary to determine the effective thermal conductivity of a granular medium are the thermal conductivity and the density of the components. In addition, the geometrical arrangement of the components in the medium must be known along with their volumetric concentration. The thermal conductivity of the particles, k_α and that of the air, k_γ, are assumed to be known. The thermal conductivity of the binder, k_β, the volume fraction of the binder, ϕ_β, and the volume fraction of the particles, ϕ_α, are the variables whose influence upon the effective thermal conductivity is to be determined.

The dominant structural characteristic is the interfacial contact area among the components. A quantitative measure of the interfacial contact area can be obtained by extending Gurland's [6] definition of contiguity between identical components to the general case for any two components. The contiguity, C_{ij}, between component i and component j is defined to be the fraction of the total interface area of component i that shares a common interface area with component j. There are four distinguishable interface areas for the α–β–γ system shown in Fig. 1. The contiguities that describe these interface areas are given by [7]

$$C_{\alpha\alpha} = \frac{2S_{\alpha\alpha}}{(2S_{\alpha\alpha} + S_{\alpha\beta} + S_{\alpha\gamma})}, \tag{1}$$

$$C_{\alpha\beta} = \frac{S_{\alpha\beta}}{(2S_{\alpha\alpha} + S_{\alpha\beta} + S_{\alpha\gamma})}, \tag{2}$$

$$C_{\alpha\gamma} = \frac{S_{\alpha\gamma}}{(2S_{\alpha\alpha} + S_{\alpha\beta} + S_{\alpha\gamma})}, \tag{3}$$

$$C_{\beta\gamma} = \frac{S_{\beta\gamma}}{(S_{\beta\alpha} + S_{\beta\gamma})}. \tag{4}$$

Examining Fig. 1 it is evident that

$$S_{\alpha\beta} = S_{\beta\alpha} \tag{5}$$

and, summing equations (1)–(3) shows that

$$C_{\alpha\alpha} + C_{\alpha\beta} + C_{\alpha\gamma} = 1. \tag{6}$$

The contiguities are key parameters because they produce a statistical analog of the boundary conditions that would be required for an exact solution to the heat conduction equation in the real granular medium.

Given a finite volume, V_T, of the granular medium illustrated in Fig. 1, the functional dependence between the effective thermal conductivity and the measureable variables can be expressed as

$$k_e = f_0(k_\alpha, k_\beta, k_\gamma, V_\alpha, V_\beta, V_\gamma, S_{\alpha\alpha}, S_{\alpha\gamma}, S_{\beta\gamma}). \tag{7}$$

The variables in equation (7) are subject to the following constraint equations:

$$V_\alpha + V_\beta + V_\gamma = V_T, \tag{8}$$

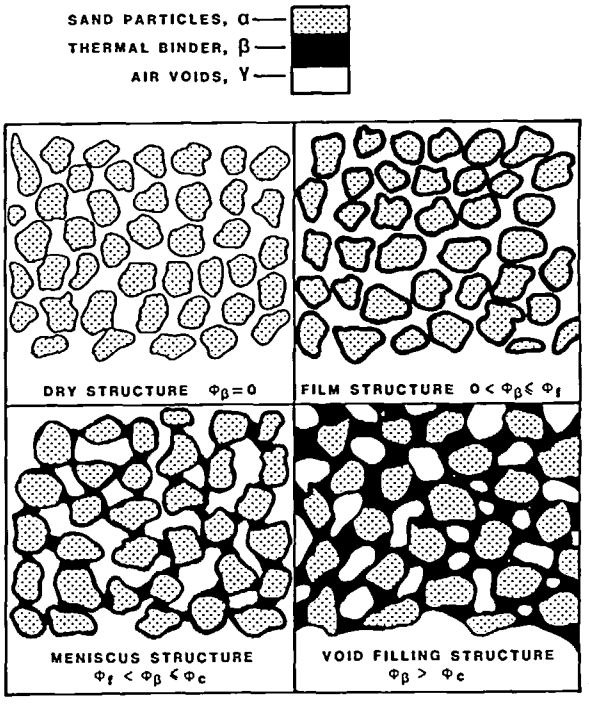

FIG. 2. Illustration of the microstructures of a three component granular material as a function of volume fraction of binder.

$$2S_{\alpha\alpha} + S_{\alpha\beta} + S_{\alpha\gamma} = S_\alpha, \quad (9)$$

$$S_{\beta\gamma} + S_{\beta\alpha} = S_\beta \quad (10)$$

and the reciprocity relation, equation (5).

In equations (9) and (10), S_α and S_β are the total interface area per unit volume of the α and β components, respectively. Selecting k, S and V as fundamental reference dimensions and using equations (8)–(10) gives the following dimensionless correlation equation:

$$\frac{k_c}{k_\alpha} = f_1\left(\frac{k_\beta}{k_\alpha}, \frac{k_\gamma}{k_\alpha}, \phi_\alpha, \phi_\beta, C_{\alpha\alpha}, C_{\alpha\beta}, \frac{S_\beta}{S_\alpha}\right) \quad (11)$$

where the volume fractions, ϕ_α and ϕ_β, are defined as

$$\phi_\alpha = \frac{V_\alpha}{V_T}, \quad (12)$$

$$\phi_\beta = \frac{V_\beta}{V_T}. \quad (13)$$

In equation (11), the thermal conductivity ratios and the volume fractions of the components can be obtained by macroscopic measurements. The dimensionless variable, S_β/S_α, can be shown to be related to the heat transfer across the β–γ interface.

An experimental determination of the function, f_1, in equation (11) is impractical because of the number of variables involved; hence, an approximate analytical model is desirable. To arrive at a physically realistic model, it is useful to examine the development of the material microstructure as the volume fraction of binder is increased from zero.

Both photomicroscopic evidence and thermal conductivity data have been obtained which demonstrate that four distinct microstructures can exist in the α–β–γ medium depending upon the volume fraction of binder [7]. These basic microstructures are illustrated in Fig. 2 and are designated by the terms: dry structure, film structure, meniscus structure and void filling structure.

For the dry structure, where $\phi_\beta = 0$, most of the heat transfer will occur in the immediate region of the apparent particle contacts because this region is the path of least thermal resistance. The actual microscopic contact area between two contiguous particles is much smaller than the apparent contact area and has been experimentally estimated [8] to be of the order of 10^{-3} that of the total particle interface area. An analogous situation occurs at the interface between any two materials because of surface roughness. A dimensionless measure of the apparent α–α contact area in the dry structure category is given by the α–α or interparticle contiguity, $C_{\alpha\alpha}$.

The initial addition of a liquid binder to the dry material results in the formation of a thin film of binder on the surface of the particles. The volume fraction of binder in this film can be related to an average film thickness, t_f, and the specific surface, S_α, of the particles by

$$\phi_\beta = t_f S_\alpha, \quad (14)$$

This structure is called the film structure and exists up to some volume fraction of the binder, ϕ_f, at which incipient formation of meniscii at the particle contacts occurs. The volume fraction, ϕ_f, will in general depend upon the surface texture of the particles, their size, and the α–β surface chemistry interaction. For the range of binder contents, $0 < \phi_\beta \leqslant \phi_f$, the thermal conductivity of the composite is essentially equal to that of the dry structure because significant interparticle thermal coupling does not occur.

The third stage of microstructural development is the meniscus structure. A dramatic increase in the effective thermal conductivity of the composite occurs in this regime, because of the formation of interparticle 'heat bridges'. The heat transfer in the meniscus structure is predominantly through the α–β interfaces as illustrated in Fig. 1. The efficiency of the α–β thermal coupling increases with both the thermal conductivity of the binder, k_β, and the α–β contiguity, $C_{\alpha\beta}$. The meniscus structure exists until the particles have become completely coupled with binder. Complete coupling occurs at a volume fraction of binder, ϕ_c, such that $C_{\alpha\beta} + C_{\alpha\alpha} = 1$. For the case of moist sands, it has been shown [7] that ϕ_c is approximately equal to 0.10.

For volumetric binder contents greater than ϕ_c, the void filling microstructure exists and the effective thermal conductivity is relatively insensitive to changes in binder content up to complete saturation with binder. De Vries' [5] data for moist sands also show that the effective thermal conductivity at saturation (which corresponds to a volumetric moisture content of about 0.4) is only about 25% greater than that for a volumetric moisture content of 0.10.

The foregoing description of the microstructure development indicates that for binders whose conductivity is much greater than that of air, the greatest increase in the effective thermal conductivity with the volumetric binder content will occur in the meniscus structure regime. Thus, the ensuing analysis will be limited to the meniscus structure where the volumetric binder content is between ϕ_f and ϕ_c.

To obtain a closed form solution for f_1 in equation (11), two fundamental simplifying assumptions are made. The first assumption involves similarity between the microscopic and macroscopic isotherms. This assumption implies that the isotherms shown in Fig. 1 are parallel planes regardless of the scale of the structure. The second assumption considers the effective thermal conductivity of the composite medium to be quantitatively described by the effective thermal conductivity of an equivalent unit cell consisting of series and parallel thermal resistors.

The equivalent unit cell takes into account the following qualitative characteristics of the heat transport:

(1) The effective thermal conductivity of the medium in the dry and film structures is primarily determined by the effective interparticle contact area.

(2) The effective thermal conductivity over and

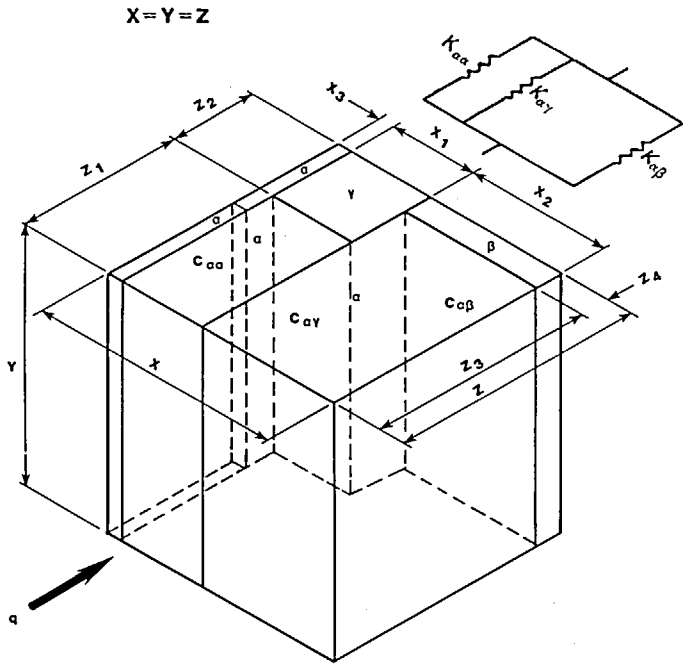

FIG. 3. Model of the equivalent unit cell of a three component granular material in the meniscus structure.

above that in the dry state is primarily determined by the thermal conductivity of the binder and the degree of α–β coupling which is quantified by the α–β contiguity.

(3) Because of the relative magnitudes of the thermal conductivity of the air and binder compared to that of the solid particles, the heat transfer across the α–γ and β–γ interfaces exerts second and third order effects, respectively, on the effective thermal conductivity of the medium.

A structural model of the unit cell that incorporates the three foregoing physical characteristics of the heat transfer is shown in Fig. 3. The equivalent unit cell consists of three parallel conductances K_{zz}, $K_{z\beta}$, and $K_{z\gamma}$ which account for the heat transfer across $\alpha-\alpha$, $\alpha-\beta$ and α–γ interfaces, respectively. Since the heat transfer across the β–γ interface exerts a third order effect, it has been assumed to be negligibly small with respect to the heat transfer across the α–α, α–β and α–γ interfaces. Because S_β/S_z accounts for the heat transfer across the β–γ interface, it can be eliminated as a significant variable in equation (11). In the limiting cases where the thermal conductivity of the binder approaches either the thermal conductivity of air or that of the particles, this approximation becomes invalid.

To illustrate the physical plausibility of the unit cell model shown in Fig. 3, consider a representative heat transport channel across the α–β interfaces as illustrated in Fig. 1. If the heat transport channel is assumed to be straightened and the individual α and β resistors are combined by the laws of series resistors, then a structure which corresponds to the $K_{z\beta}$ conductance of Fig. 3 will result. An analogous line of reasoning may be used to obtain the K_{zz} and $K_{z\gamma}$ conductances. Combining the individual conductances shown in Fig. 3 gives the following expression for the effective thermal conductivity of the unit cell [7]:

$$\frac{k_e}{k_z} = \frac{X_3}{X} + \frac{\left(\frac{X_2}{X}\right)^2}{\frac{X_2}{X} - \phi_\beta + \frac{k_z}{k_\beta}\phi_\beta} + \frac{\left(\frac{X_1}{X}\right)^2}{\frac{X_1}{X} - \phi_\gamma^* + \frac{k_z}{k_\gamma}\phi_\gamma^*} \quad (15)$$

where ϕ_γ^* is the volume fraction of air that is in series with the particles.

Recognizing that the heat transfer is in the direction shown in Fig. 3, and using the definition of contiguity, equation (15) becomes

$$\frac{k_e}{k_z} = C_{zz} + \frac{C_{z\beta}^2}{C_{z\beta} - \phi_\beta + \frac{k_z}{k_\beta}\phi_\beta} + \frac{C_{z\gamma}^2}{C_{z\gamma} - \phi_\gamma^* + \frac{k_z}{k_\gamma}\phi_\gamma^*}. \quad (16)$$

Using the approximations

$$\phi_\gamma^* = \phi_\gamma \quad \text{for } C_{z\beta} = 0$$

and

$$\phi_\gamma^* = 0 \quad \text{for } C_{z\beta} = 1 - C_{zz},$$

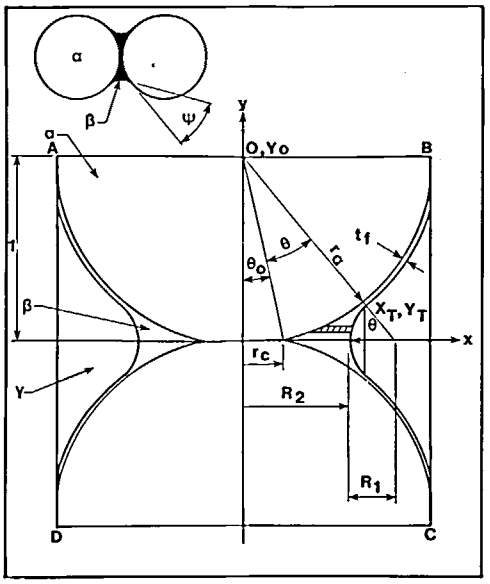

FIG. 4. Model of the α–β interface at a particle contact.

and using a linear interpolation between $C_{z\beta} = 0$ and $C_{z\beta} = 1 - C_{zz}$ gives

$$\phi_\gamma^* = \phi_\gamma\left(1 - \frac{C_{z\beta}}{1 - C_{zz}}\right). \tag{17}$$

Equation (16) should also approximately satisfy the two limiting conditions

$$k_e = k_d \quad \text{for } \phi_\beta = 0$$

and

$$k_e \to k_d \quad \text{as } k_\beta \to k_\gamma$$

where k_d is the thermal conductivity of the granular medium without any binder. For the case of a medium with no binder present, $C_{z\beta} = 0, \phi_\beta = 0$, and equation (16) can be solved for C_{zz} to give

$$C_{zz} = \frac{\frac{k_d}{k_z}\left[1 - \phi_\gamma + \frac{k_z}{k_\gamma}\phi_\gamma\right] - 1}{\frac{k_d}{k_z} - 1 - \phi_\gamma + \frac{k_z}{k_\gamma}\phi_\gamma}. \tag{18}$$

If k_d is a known empirical or analytical function of ϕ_γ and k_z/k_γ, then an effective value of C_{zz} can also be determined as a function of these variables from equation (18). Numerous analytical formulae are available in the literature [9–12] which give k_d as a function of ϕ_γ and k_z/k_γ.

The second limiting condition will not be satisfied exactly with the proposed model because the approximation of negligible heat transfer across the β–γ interface is not strictly valid when $k_\beta \to k_\gamma$. This conditioned can be better satisfied if k_β in equation (16) is replaced by $k_\beta - k_\gamma$. Thus, equation (16) becomes

$$\frac{k_e}{k_z} = C_{zz} + \frac{C_{z\beta}^2}{C_{z\beta} - \phi_\beta + \frac{k_z\phi_\beta}{k_\beta - k_\gamma}} + \frac{C_{z\gamma}^2}{C_{z\gamma} - \phi_\gamma^* + \frac{k_z}{k_\gamma}\phi_\gamma^*}. \tag{19}$$

To obtain a solution to equation (19) now requires that $C_{z\beta}$ be determined as a function of ϕ_β and ϕ_γ for a given medium. To determine this function, the α–β and α–γ interfaces at representative particle contact point are examined.

A representative α–β interface is assumed to be geometrically described by the spherical particle model shown in Fig. 4. To account for the effective interparticle contiguity, C_{zz}, the spherical particles are assumed to be truncated at their point of contact [4]. The circular area of contact between two particles, A_{zz}, is given by

$$A_{zz} = \pi r_c^2 \tag{20}$$

The binder, β, is assumed to occupy a uniform thin film of equivalent thickness, t_f, on the surface of the spheres and a circular ring at the contact points. In general, the wetting angle, ψ, between the binder and particles will depend upon the interfacial surface energies among the α, β and γ components. However, for the purposes of this study, the wetting angle is assumed to be zero; that is, the binder perfectly wets the particles. For perfect wetting, it has been demonstrated [13] that the circular meniscus approximates the actual meniscus to within about 1.5%.

After significant mathematical manipulation, it can be shown that for $t_f/r_z \ll 1$ the volume of revolution of the meniscus, $V_{c\beta}$, is given by [7]

$$\frac{V_{c\beta}}{r_z^3} = 2\pi\cos\theta_0\left\{\left[\frac{\cos\theta_0}{\cos\theta} - 1\right]^2\left[1 - \left(\frac{\pi}{2} - \theta\right)\tan\theta\right]\right\} \tag{21}$$

where

$$\theta_0 = \sin^{-1}\left(\frac{r_c}{r_z}\right), \tag{22}$$

$$\theta = \sin^{-1}\left(\frac{x_T}{r_z}\right).$$

In this case, the volume of binder per contact, $V_{c\beta}$, is also given by

$$\frac{V_{c\beta}}{r_z^3} = \frac{8\pi\phi_\beta}{3N\phi_z} \tag{23}$$

where N is number of contacts per particle. Substitution of equation (23) into equation (21) gives

$$\frac{4\phi_\beta}{3N\phi_z} = \cos\theta_0\left\{\left[\frac{\cos\theta_0}{\cos\theta} - 1\right]^2\left[1 - \left(\frac{\pi}{2} - \theta\right)\tan\theta\right]\right\}. \tag{24}$$

The contiguities, C_{zz} and $C_{z\beta}$, for the model shown in Fig. 4 are given by the following expressions [7]:

$$C_{zz} = \frac{N}{4}\left(\frac{r_c}{r_z}\right)^2, \tag{25}$$

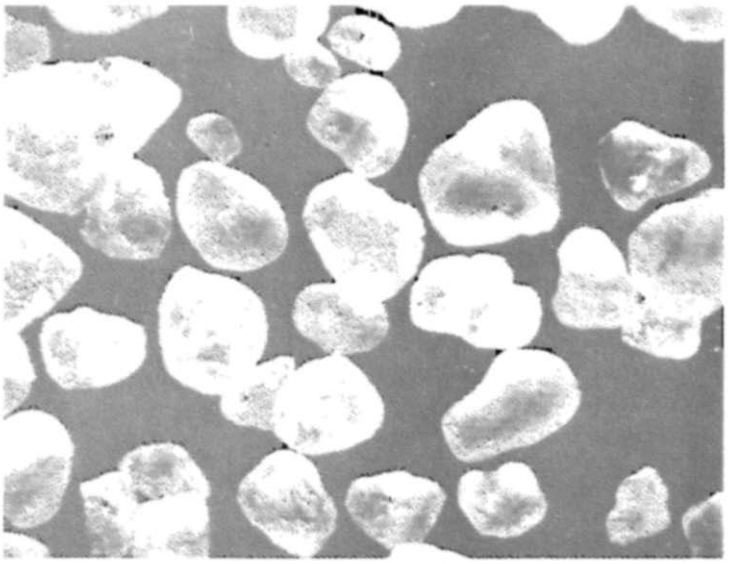

FIG. 5(a). Stereo-photomicrograph of ASTM C-109 Ottawa sand particles, ×40.

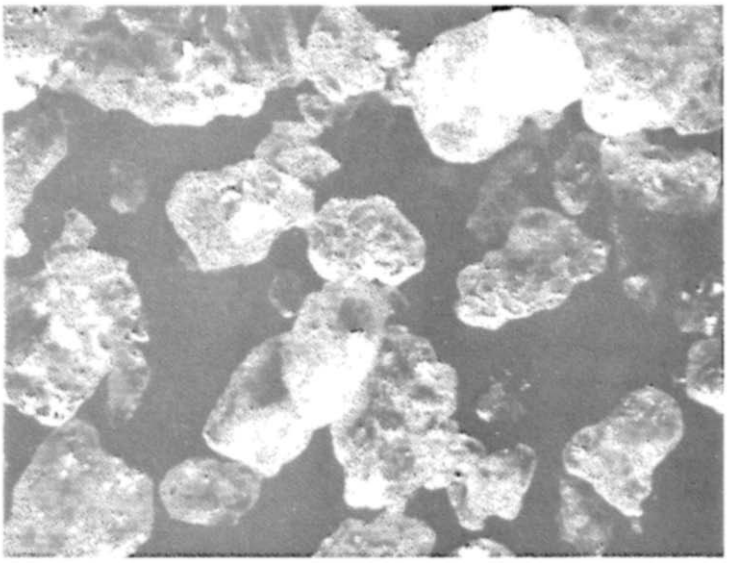

FIG. 5(b). Stereo-photomicrograph of masonry-type sand particles, ×30.

$$C_{\alpha\beta} = \frac{N}{2}\left\{\left[1 - \left(\frac{r_c^2}{r_\alpha}\right)\right]^{1/2} - \cos\theta\right\}, \quad (26)$$

$$C_{\alpha\beta} = \frac{N}{2}\left\{\left[1 - \frac{4C_{\alpha\alpha}}{N}\right]^{1/2} - \cos\theta\right\}. \quad (27)$$

The number of contacts per particle, N, depends upon the packing arrangement which is a function of the volume fraction of particles. The three fundamental packing arrangements for uniform spheres are simple cubic, body centered cubic, and face centered cubic. The values of ϕ_α and N for these packing arrangements are $\pi/6$, 0.68 and 0.74 and 6, 8, and 12 respectively. Using these points, the following hyperbolic interpolating equation can be used to estimate N as a function of ϕ_α:

$$N = \frac{\phi_\alpha - \pi/6}{0.5550 - 0.7017\,\phi_\alpha} + 6. \quad (28)$$

Equations (21)-(28) can now be used to calculate the dimensionless effective thermal conductivity of the unit cell. The detailed calculation procedure is described in ref. [7] and can be performed with a programmable calculator. The results of these calculations can be represented in dimensionless form as

$$\frac{k_e}{k_\alpha} = f_2\left(\frac{k_\beta}{k_\alpha}, \frac{k_\gamma}{k_\alpha}, \phi_\alpha, \phi_\beta\right). \quad (29)$$

For a sand-like medium comprised of quartzitic particles, k_γ/k_α is constant and a 2-dim. graph can be constructed to show the functional relation among any

three of the other dimensionless variables in equation (29).

EXPERIMENTAL APPARATUS AND PROCEDURE

The thermal conductivity data used to verify the predictive accuracy of the unit cell model were obtained by the transient, 'thermal needle' technique because this method requires relatively simple instrumentation and it provides accurate results in a relatively short time. The needle measurement is based upon the rate of temperature rise of an infinitely-long, line heat source which is embedded with negligible contact resistance in an infinite, homogeneous, isotropic and isothermal medium. The needle is introduced into the medium and is supplied with a constant heat input per unit length, q'. The temperature rise, θ, of a thermocouple located adjacent to the heating element at the center of the needle is measured as a function of time. The thermal conductivity of the adjacent medium is related to the temperature rise of the needle at two times, t_1 and t_2, after the initial thermal transients have disappeared by the equation [14, 15]

$$k = \frac{q'}{4\pi}\left[\frac{\ln (t_2/t_1)}{\theta_2 - \theta_1}\right]. \quad (30)$$

A thermal needle was designed and constructed along with the ancillary equipment to control the power and measure the temperature response of the needle. A detailed description of the thermal conductivity measurement system is given in ref. [7]. For the particular needle design used in this investigation, deterministic errors were no greater than approximately 2%.

Thermal conductivity measurements were made on two basically different types of sand-like granular materials. The first used a graded, ASTM-C-109 Ottawa sand and the second, a naturally occurring, 'masonry-type' sand. As shown in the photomicrographs of Fig. 5, the Ottawa sand particles are well-rounded whereas the masonry sand particles can be classified as subangular.

The method of quantitative stereology was used to verify the accuracy of the analytical expressions [equations (21)–(27)] used to calculate the particle–binder contiguity, ($C_{\alpha\beta}$). In order to measure the α–β contiguity as a function of the volumetric binder content, specimens were prepared for quantitative microscopic analysis. First, a fluid, epoxy binder was mixed with the sand and the mixture was compacted to the desired bulk density. The epoxy was allowed to cure and then the specimen was vacuum-impregnated with a thermosetting acrylic resin to fill the air voids. Thus, these voids were replaced by the acrylic resin and the sample could then be polished and viewed under an optical measuring microscope. After the acrylic impregnant had cured, the specimen was sawed into disks with a diamond wafering blade and polished.

Following a method described by Underwood [16], the α–β and α–γ contiguities are calculated from

$$C_{\alpha\beta} = \frac{(P_L)_{\alpha\beta}}{(P_L)_{\alpha\beta} + (P_L)_{\alpha\gamma}}, \quad (31)$$

$$C_{\alpha\gamma} = \frac{(P_L)_{\alpha\gamma}}{(P_L)_{\alpha\beta} + (P_L)_{\alpha\gamma}} \simeq 1 - C_{\alpha\beta} \quad (32)$$

where $(P_L)_{ij}$ is the number of i–j intersections encountered per unit length of test line on a section of microstructure. The relative error in estimating $C_{\alpha\beta}$ by the quantitative stereology technique is estimated to be about 5%.

RESULTS AND DISCUSSION

Figures 6–8 show the various functional relationships between the variables in equation (29). In these calculations, the thermal conductivity of the sand particles, k_α, is taken to be the average value for quartz, 8.54 W m^{-1} K^{-1}, as recommended by DeVries [5] and the density, ρ_α, of the sand particles is 2650 kg m^{-3}. The thermal conductivity, k_γ, and density, ρ_γ, of dry air at 298 K and 1.013 × 10^5 Pa are 0.0254 W m^{-1} K^{-1} and 1.2 kg m^{-3}, respectively. The interparticle contiguity, $C_{\alpha\alpha}$ is calculated from equation (18) using the following experimentally determined equation for k_d for the sands studied [7]:

$$k_d = -0.323 + 1.180\phi_\alpha (0.57 < \phi_\alpha \leqslant 0.66). \quad (33)$$

Figure 6 shows the dimensionless effective thermal conductivity as a function of the volume fraction of binder with the dimensionless thermal conductivity of the binder as a parameter. These curves show that the dimensionless effective thermal conductivity increases rapidly with the volume fraction of binder at the lower binder contents. However, the rate of increase in the dimensionless effective thermal conductivity with the volume fraction of binder decreases as the volume fraction of binder increases. A physical interpretation of this behavior can be obtained by examining the relation between the α–β contiguity and the volume fraction of binder. Figure 9 shows the theoretical α–β

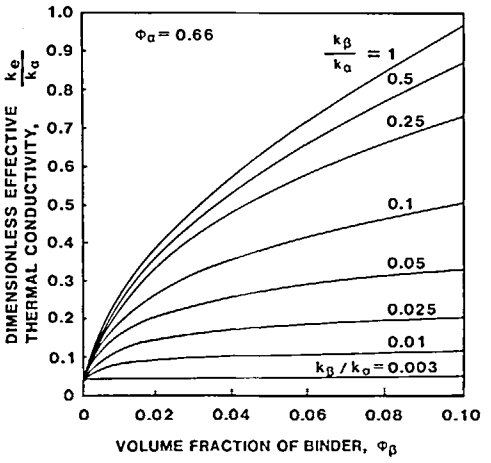

FIG. 6. Unit cell predictions for dimensionless effective thermal conductivity as a function of the volume fraction of the binder.

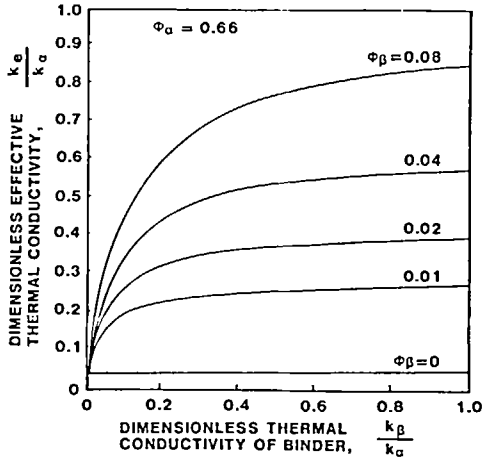

FIG. 7. Unit cell predictions for dimensionless effective thermal conductivity as a function of the dimensionless thermal conductivity of the binder.

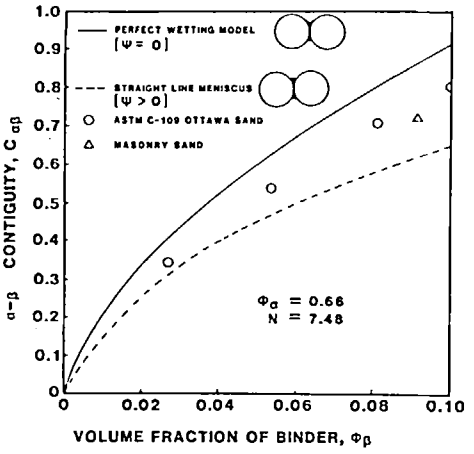

FIG. 9. Comparison of the theoretical values of the α–β contiguity with those obtained from quantitative microscopic measurements.

contiguity, $C_{\alpha\beta}$, as a function of the volume fraction of binder for the perfect wetting meniscus and for a straight line meniscus for the case where $t_f = 0$. Also shown in Fig. 9 are experimental values of $C_{\alpha\beta}$ as determined from the quantitative microscopic measurements. It is seen from Fig. 9 that the experimental data fall within about 10% of the theoretical values calculated from either meniscus model. Figure 9 shows that the initial addition of the binder has a significant influence on the α–β thermal coupling area, but, as the volume fraction of binder approaches 0.10, further increases in the coupling area, $C_{\alpha\beta}$, with the volume fraction of the binder become insignificant. Thus, the increase in the effective thermal conductivity with the addition of binder also becomes low as $C_{\alpha\beta} \to 1$. Figure 6 shows that the amount by which the dimensionless effective thermal conductivity increases with an increase in the volume fraction of binder also increases with an increase in the dimensionless thermal conductivity of the binder. This behavior is to be expected because the thermal resistance of the α–β thermal coupling decreases with an increase in the thermal conductivity of binder.

Figure 6 also shows that all of the curves converge to a common value equal to k_d/k_α as the volume fraction of binder approaches zero. Therefore, the physical requirement that

$$k_e = k_d \quad \text{for } \phi_\beta = 0$$

is satisfied. It is also evident that as the value of the thermal conductivity of the binder approaches that of air ($k_\beta/k_\alpha \to k_\gamma/k_\alpha = 0.003$), the dimensionless effective thermal conductivity approaches the value of k_d/k_α for all values of the volume fraction of the binder. Thus, the limiting condition that

$$k_e \to k_d \quad \text{for } k_\beta \to k_\gamma$$

is also satisfied.

A third limiting condition occurs when the thermal conductivity of the binder is equal to that of the particles; that is, $k_\beta/k_\alpha = 1$. In this case, the unit cell model should approximately agree with the existing two-component models for which the α component forms a continuous matrix within which the discrete γ component is interspersed. Francl and Kingery [17] conducted an experimental investigation for such 'porous' materials and concluded that Loeb's [18] equation was the best fit to the data. For the case where the air voids are isodimensional and the mean temperatures of the medium is about 298 K, Loeb's equation reduces to

$$\frac{k_e}{k_\alpha} = 1 - \phi_\gamma = 1 - (\phi_\alpha + \phi_\beta). \tag{34}$$

The values predicted by the unit cell model are lower than those predicted by Loeb's equation for volumetric binder contents less than about 0.065 and higher for binder contents greater than about 0.065. The maximum difference between the two models is about 25% at a volumetric binder content equal to

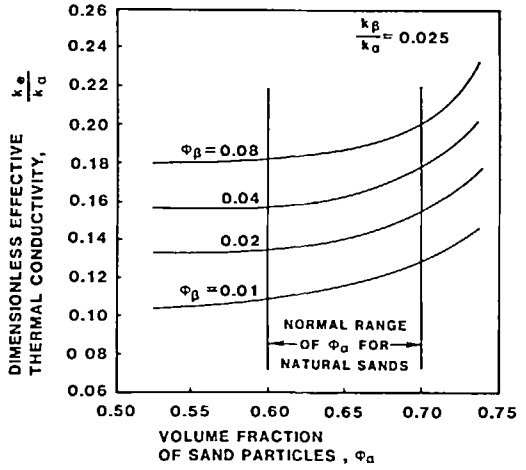

FIG. 8. Unit cell predictions for dimensionless effective thermal conductivity as a function of the volume fraction of sand particles.

0.10. Such a difference between these two models is to be expected because the material structures represented by the respective models become quite different at these extreme values of the volumetric binder contents and thermal conductivities. For example, if the volume fraction of binder is equal to zero, then the unit cell model predicts the effective thermal conductivity of a sand-like granular material whereas Loeb's equation predicts that of a cemented 'brick-like' material. Also, for the case where the thermal conductivity of binder is equal to that of the particles, the unit cell model's approximation of negligible heat transfer through the β–γ interface is no longer valid.

Figure 7 shows the dimensionless effective thermal conductivity as a function of the dimensionless thermal conductivity of the binder with the volume fraction of the binder as a parameter. These curves show that the dimensionless effective thermal conductivity increases at a decreasing rate with an increase in the dimensionless thermal conductivity of the binder.

For media used in commercial applications such as sand casting or thermal backfill materials with a given volume fraction of binder, the maximum practical value of the dimensionless effective thermal conductivity will occur at a value for the dimensionless thermal conductivity of the binder of less than unity. Using this value as a reference, it is seen from Fig. 7 that a larger percentage of the increase in the dimensionless effective thermal conductivity occurs for values of the dimensionless thermal conductivity of the binder less than about 0.1. For example, at a volume fraction of binder of about 0.08, the dimensionless effective thermal conductivity attains a value equal to one-half its maximum at a value of the dimensionless thermal conductivity of the binder of about 0.09.

Figure 8 shows the dimensionless effective thermal conductivity as a function of the volume fraction of the sand particles for a constant dimensionless thermal conductivity of the binder. For the range of the volume fraction of sand particles normally encountered in natural sands, $0.6 \leqslant \phi_\alpha \leqslant 0.7$, Fig. 8 shows that the

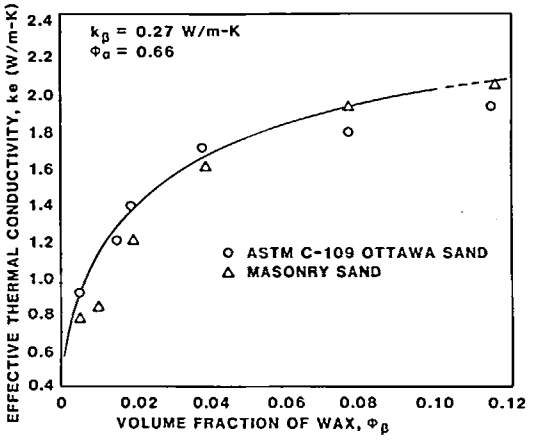

FIG. 10. Comparison of unit cell model prediction with experimental data for wax-sand mixtures.

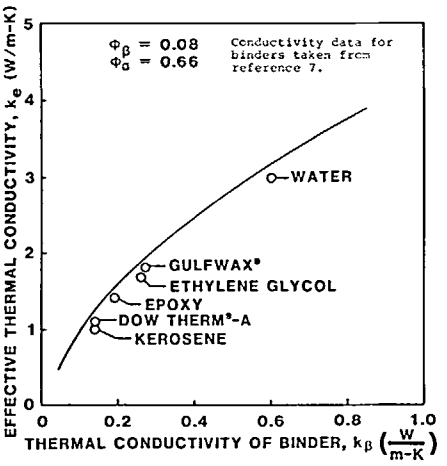

FIG. 11. Effect of the thermal conductivity of the binder on the effective thermal conductivity of sand.

dimensionless effective thermal conductivity increases only moderately with an increase in the volume fraction of the sand particles. Moreover, for the range of volumetric binder contents, $0.01 \leqslant \phi_\beta \leqslant 0.08$, the increase in the dimensionless effective thermal conductivity with the volume fraction of sand particles is seen to be about the same at all values of the volumetric binder content. This theoretical result agrees with the experimental observations of Kersten [19].

The effective thermal conductivity of the ASTM-C-109 Ottawa sand and the masonry sand was measured as a function of the volumetric binder content for a binder consisting of Gulfwax® which has a thermal conductivity of about 0.27 $W\,m^{-1}\,K^{-1}$. This value was measured with a thermal probe and verified with literature values [7]. For the samples consisting of wax binders, the molten wax was mixed with the sand at a temperature of about 343 K, and the probe was inserted into the hot mixture immediately after compaction. The specimens were compacted to a dry bulk density of about 1750 $kg\,m^{-3}$ (ϕ_α = 0.66). As the specimen cooled, it shrank tightly around the probe due to the solidification of the wax. Therefore, for the wax mixtures, the possibility of an error caused by contact resistance between the probe and the specimen was minimized, if not eliminated. For the wax mixtures, Fig. 10 shows that the unit cell model predictions agree with the experimental data over the entire range of volumetric binder contents to within about 10%.

The effective thermal conductivity of the ASTM-C-109 Ottawa sand was also measured for several different binders at a volumetric binder content equal to about 0.08. Figure 11 shows a comparison between the theoretical values as predicted by the unit cell model and the experimental data [7]. The theoretical curve is about 10% greater than the experimental data for the sand containing the liquid binders whereas the agreement is much better for the solid binders. This difference can possibly be attributed to both the

contact resistance at the probe–specimen interface and imperfect wetting between the sand and the fluid binders. It should be noted that in order to accurately measure the effective thermal conductivity of specimens which contain a liquid binder particular attention must be given to the effects of contact resistance and liquid migration away from the heat source. For example, Hartley's [20] soil thermal stability studies have shown that the measured value of the effective thermal conductivity in the meniscus regime can be up to 50% low if the probe heat flux results in significant migration of the water away from the heat source. Because of a lower contact resistance, the cemented specimens (those specimens which contain binders that solidify after mixing) will have a higher effective thermal conductivity than the uncemented specimens which have liquid binders assuming other factors are unchanged.

APPLICATION OF THE UNIT CELL MODEL

The results obtained from the unit cell model have practical applications to design of thermal backfill materials having enhanced thermal conductivity. Both the model and the experimental data demonstrate that the best way to increase the effective thermal conductivity of a given sand-like granular material is to thermally couple contiguous sand grains with a thermal binder whose thermal conductivity is 'high' with respect to that of air. A measure, $n_{\alpha\beta}$, of the efficiency of the α–β thermal coupling is provided by the second term in equation (19) because it describes the heat transfer through the α–β interface. Thus

$$n_{\alpha\beta} = \frac{C_{\alpha\beta}^2}{C_{\alpha\beta} - \phi_\beta \dfrac{k_\alpha}{k_\beta - k_\gamma}\phi_\beta} \qquad (35)$$

When the particles are completely coupled with a binder whose thermal conductivity is equal to that of the particles, $C_{\alpha\beta} = 1 - C_{\alpha\alpha}$, $k_\beta/k_\alpha = 1$ and the value of $n_{\alpha\beta}$ is essentially equal to unity. On the other hand, if the value of the thermal conductivity of the binder is equal to that of air, then the value of $n_{\alpha\beta}$ is equal to zero. For a given binder, the maximum value of $n_{\alpha\beta}$ will occur when the α–β contiguity is a maximum. The maximum value of the α–β contiguity is equal to $1 - C_{\alpha\alpha}$, and this maximum is achieved for sands at volumetric binder contents in the neighbourhood of 0.10. Therefore, the addition of a thermal binder in excess of about 10% by volume will produce only a minimal increase in the value of $n_{\alpha\beta}$ and thus will probably not be cost effective for increasing the effective thermal conductivity of the composite.

In regard to the thermal conductivity of the binder, it was shown that for a given volumetric binder content the dimensionless effective thermal conductivity of the composite will be equal to about one-half its maximum value when the value of the dimensionless thermal conductivity of the binder is about 0.10. If the binder is water, then the value of k_β/k_α is about 0.07. Because water has the highest thermal conductivity of the nonmetallic liquids, the value of 0.10 for k_β/k_α appears to be an upper practical limit when sand is used as a base material. Substituting values of 1, 0.10, and 0.10, for $C_{\alpha\beta}$, ϕ_β and k_β/k_α respectively, equation (35) gives an upper practical limit of about 0.5 for $n_{\alpha\beta}$. In comparison, for the example of a moist sand containing about 10% water by volume, the value of $n_{\alpha\beta}$ is about 0.4. Therefore, for a thermal backfill material to be technologically effective, it need not contain more than about ten percent by volume of a binder whose thermal conductivity is about one-tenth that of the sand particles.

CONCLUSIONS

The foregoing analytical and experimental study of the effective thermal conductivity of a granular medium comprised of sand particles, a thermal binder and air has shown the following:

(1) The stereological concept of contiguity can be used to quantitatively relate the macroscopic effective thermal conductivity of a composite granular medium to the microscopic interfacial contact area among its components.

(2) Four basic microstructures occur in a sand-like granular medium as the volume fraction, ϕ_β, of a liquid binder is increased from zero. These microstructures can be classified into the following basic categories:

dry structure	$\phi_\beta = 0$,
film structure	$0 < \phi_\beta \leqslant \phi_f$,
meniscus structure	$\phi_f < \phi_\beta \leqslant \phi_c$,
void filling structure	$\phi_\beta > \phi_c$.

(3) The particle–binder contiguity, $C_{\alpha\beta}$, which is defined as the fraction of total interface area of sand particles, α, that is commonly shared with the binder, β, provides a quantitative measure of the degree of thermal coupling between the particles and binder. The particle–binder contiguity, $C_{\alpha\beta}$, can be accurately calculated by the analysis of a representative contact between two particles, or measured from a microstructural section plane of the material. The analytical expression for $C_{\alpha\beta}$ can be used in a relatively simple unit cell model comprised of thermal resistors to calculate the effective thermal conductivity of the medium. The unit cell model accurately predicts the effective conductivity in the meniscus structure as a function of the thermal conductivity of the components and their volumetric concentration once the effective thermal conductivity of the composite containing zero binder is known. The zero binder content conductivity can be determined experimentally or analytically from numerous formulae presently available in the literature.

(4) The greatest increase in the effective thermal conductivity of a sand-like granular medium occurs in the meniscus structure regime where the sand particles become thermally coupled with binder.

(5) The efficiency of the heat transfer across the particle–binder interface can be expressed by a dimensionless parameter, $n_{s\beta}$, which takes into account the combined effect of the particle–binder contiguity, $C_{s\beta}$, and the thermal conductivity, k_β of the binder.

(6) The unit cell model provides practical design guidelines for the formulation of thermal backfill materials used to increase the rate of heat transfer between a buried heat source or sink and the earth. Given present economic and material constraints for thermal backfill applications, the maximum practical value for $n_{s\beta}$ is about 0.5. This occurs when the sand contains about 10% by volume of a binder whose thermal conductivity is about 10% of that of the sand particles.

REFERENCES

1. J. C. Maxwell, *A Treatise on Electricity and Magnetism*, Vol. 1, p. 440. Oxford University Press, London (1892).
2. Lord Rayleigh, On the influence of obstacles arranged in rectangular order upon the properties of a medium, *Phil. Mag.* **34**, 481–502 (1892).
3. A. Eucken, Wärmeleitfahigkeit keramischer feuerfester Stoffe; Berechnuglaus der Wärmeleitfahigkeit der Bestandteile, *Forsch. Geb. InWes.* B3, Forschungsheft No. 353 (1932).
4. A Gemant, The thermal conductivity of soils, *Appl. Phys.* **21**, 750–752 (1950).
5. D. A. de Vries and N. H. Afgan, *Heat and Mass Transfer in the Biosphere*, Part 1, *Transfer Processes in the Plant Environment*, pp. 211–235. Wiley, Washington, D.C. (1975).
6. J. Gurland, The measurement of grain contiguity in two phase alloys, *Trans. Am. Inst. Min. Metall., Pet. Eng.* **212**, 452–455 (1958).
7. K. W. Jackson, Enhancement of thermal energy transport through granular media, Ph.D. Thesis, Georgia Inst. of Tech. (1980).
8. W. Woodside and J. H. Messmer, Thermal conductivity of porous media, I, Unconsolidated sands, *Appl. Phys.* **32**, 1688–1699 (1961).
9. A. D. Brailsford and K. G. Mayor, The thermal conductivity of aggregates of several phases, including porous materials, *Br. J. Appl. Phys.* **15**, 313–319 (1964).
10. D. Kunii and J. M. Smith, Heat transfer characteristics of porous rocks, *A.I.Ch.E. Jl* **6**, 71–77 (1960).
11. R. Krupiczka, Analysis of thermal conductivity in granular materials, *Int. Chem. Engng* **7**, 122–143 (1967).
12. M. Van Rooyen, Soil thermal resistivity, Ph.D. Thesis, Princeton University (1959).
13. R. A. Fisher, On the capillary forces in an ideal soil; Correction of formulae given by W. B. Haines, *Agric. Sci.* **16**, 492–505 (1926).
14. H. S. Carslaw and J. C. Jaeger, *Conduction of Heat in Solids*, pp. 261–262. Oxford University Press (1959).
15. F. C. Hooper and F. R. Lepper, Transient heat flow apparatus for the determination of thermal conductivities, *Heat Piping Air Cond.* **22**, 129–134 (1950).
16. E. E. Underwood, *Quantiative Stereology*. Addison Wesley (1970).
17. J. Francl and W. D. Kingery, Thermal conductivity: IX, experimental investigation of effect of porosity on thermal conductivity, *Am. Ceram Soc.* **37**, 99–107 (1954).
18. A. L. Loeb, Development of thermal conductivity expression for special case of prolate spheroids, *Am. Ceram. Soc.* **37**, 96 (1954).
19. M. S. Kersten, Thermal properties of soils, *Univ. Minn. Inst. Tech. Bul.* 28 (1949).
20. J. G. Hartley and W. Z. Black, Transient, simultaneous heat and mass transfer in moist, unsaturated soils, *Trans. Am. Soc. Mech. Engrs*, Series C, *J. Heat. Transfer* **103**, 376–382 (1981).

UN MODELE DE CELLULE UNIQUE POUR PREDIRE LA CONDUCTIVITE THERMIQUE D'UN MILIEU GRANULAIRE CONTENANT UN LIANT ADHESIF

Résumé—Un modèle de cellule unique est proposé pour prédire la conductivité thermique effective d'un milieu granulaire composé de sable, d'un liant thermique et d'air. Ce modèle est décrit par les trois conductances thermiques dominantes qui tiennent compte du transfert thermique à travers les interfaces entre les composants. Le concept stéréologique de contriguïté est utilisé pour relier quantitativement la conductivité macroscopique effective à la surface de contact microscopique entre les composants. En utilisant un modèle de contact entre deux particules, on développe une expression analytique de la contiguïté. Cette expression est utilisée dans le modèle de la cellule pour calculer la conductivité thermique effective du milieu en fonction de la conductivité thermique des composants et de leur concentration volumique. La précision de l'estimation est vérifiée avec des mesures microscopiques nombreuses et des données obtenues avec la technique transitoire sur éprouvette cylindrique.

Le modèle de cellule est appliqué au dessin des matériaux de remplissage. L'analyse et l'expérience montrent toutes deux que le couplage thermique des particules de sable contigües avec un liant peut accroître sensiblement la conductivité effective du sable sec. On identifie quatre régimes de microstructure et ces régimes sont reliés quantitativement à la fraction volumique du liant. Le plus grand accroissement de la conductivité thermique en fonction de la fraction volumique du liant apparait lorsque les particules de sable deviennent thermiquement couplées au liant. Le modèle fournit des régles quantitatives pour la conductivité et la fraction de volume du liant qui sont utilisables pour réaliser le plus grand accroissement de la conductivité thermique du sable sec. Ainsi les résultats de cette étude ont une application pratique pour accroître le transfert thermique entre la terre et les sources de chaleur comme des cables électriques de puissance et des serpentins de pompe à chaleur.

EIN EINHEITSZELLENMODELL ZUR BERECHNUNG DER WÄRMELEITFÄHIGKEIT EINES KÖRNIGEN MEDIUMS MIT ADHESIVEN BINDEMITTELN

Zusammenfassung—Es wird ein Einheitszellenmodell vorgestellt, welches zur Berechnung der effektiven Wärmeleitfähigkeit eines körnigen Mediums, das aus Sandpartikeln, einem thermischen Bindemittel und Luft besteht, verwendet werden kann. Das Einheitszellenmodell wird durch drei dominante Wärmeleitfähigkeiten beschrieben, die für den Wärmetransport zwischen den Oberflächen der Komponenten des Mediums verantwortlich sind. Das stereologische Berührungskonzept wird verwendet um die makroskopische, effektive Wärmeleitfähigkeit mit dem mikroskopischen Flächenkontakt zwischen den Komponenten zu verketten. Unter Anwendung des geometrischen Modells eines repräsentativen Kontakts zwischen zwei Partikel wird ein analytischer Ausdruck für die Berührung gefunden. Dieser Ausdruck wird im Einheitszellenmodell dazu benutzt, die effektive Wärmeleitfähigkeit des Mediums in Abhängigkeit der Wärmeleitfähigkeiten der Komponenten und ihrer Volumenanteile zu berechnen. Die Rechengenauigkeit des Einheitszellenmodells für sandartige Stoffe wird durch zahlreiche quantitative, mikroskopische Messungen und Wärmeleitfähigkeitsdaten, die mit der instationären Zylindermethode erhalten wurden, nachgewiesen.

Das Einheitszellenmodell wird auf die Formgebung von thermischem Auffüllmaterial angewendet. Sowohl die Berechnungen als auch die Experimente zeigen, daß durch thermische Kopplung angrenzender Sandpartikel mit einem Bindemittel die effektive Wärmeleitfähigkeit von Sand bedeutend erhöht werden kann. Vier grundsätzliche mikrostrukturelle Bereiche des Mediums wurden erkannt und quantitativ auf den Volumenanteil des Bindemittels bezogen. Die größte Zunahme der effektiven Wärmeleitfähigkeit bezogen auf den Volumenanteil des Bindemittels zeigt sich in einem Bereich, in dem die Sandpartikel durch das Bindemittel thermisch gekoppelt werden. Das Einheitszellenmodell stellt quantitative Richtlinien für die Wärmeleitfähigkeit und den Volumenanteil des Bindemittels auf, die benutzt werden können, um die größte Zunahme der effektiven Wärmeleitfähigkeit von trockenem Sand zu erhalten. Daher finden die Ergebnisse dieser Untersuchung praktische Anwendung bei der Entwicklung und Formgebung von thermischem Auffüllmaterial zur Erhöhung des Wärmetransports zwischen dem Erdreich und unterirdischen Wärmequellen, wie z.B. Erdkabel und Erdwärmepumpen.

МОДЕЛЬ ЕДИНИЧНОЙ ЯЧЕЙКИ ДЛЯ РАСЧЕТА ТЕПЛОПРОВОДНОСТИ ГРАНУЛИРОВАННОЙ СРЕДЫ, СОДЕРЖАЩЕЙ КЛЕЙКОЕ СВЯЗУЮЩЕЕ ВЕЩЕСТВО

Аннотация—Предложена модель единичной ячейки, которая может использоваться для расчета эффективной теплопроводности гранулированной среды, состоящей из частиц песка, термического связующего и воздуха. Модель единичной ячейки описывается тремя составляющими теплопроводности, учитывающими перенос тепла через границы раздела компонентов среды. Используется стереологическое понятие смежности для установления количественной связи макроскопической эффективной теплопроводности с микроскопической межфазной площадью контакта между компонентами среды. На основе геометрической модели характерного контакта между двумя частицами получено аналитическое выражение для смежности. Это выражение используется в модели единичной ячейки для расчета эффективной теплопроводности среды как функции теплопроводности компонентов и их объемной концентрации. Точность модели единичной ячейки для сред типа песка проверена с помощью большого ряда количественных микроскопических измерений и данных по теплопроводности, полученных нестационарным методом цилиндрического датчика.

Модель единичной ячейки используется для расчета термических свойств материалов засыпок. Как анализ, так и эксперимент показывают, что частицы песка, термически взаимодействующие со связующим, могут существенно увеличить эффективную теплопроводность сухого песка. Выделены четыре основных микроструктурных режима среды и установлена количественная зависимость этих режимов от объемной доли связующего. Показано, что максимальное увеличение эффективной теплопроводности с увеличением объемной доли связующего происходит в режиме, когда частицы песка термически взаимодействуют со связующим веществом. Модель единичной ячейки позволяет получить количественную связь теплопроводности и объемной доли связующего, которую можно использовать для определения максимального увеличения эффективной теплопроводности сухого песка. Таким образом, результаты исследования могут использоваться на практике для расчета и получения материалов засыпок, которые могли бы увеличить интенсивность теплопереноса между грунтом и такими погруженными в него тепловыми источниками, как например, электрические кабели и змеевики тепловых насосов.